IEEE Open Journal of
Vehicular Technology

Received 2 March 2020; accepted 24 March 2020. Date of publication 3 April 2020;
date of current version 6 May 2020. The review of this article was arranged by Associate Editor Y. Ko.

Digital Object Identifier 10.1109/OJVT.2020.2984753

Regularized WDFDC Receivers for Selective Detect-and-Forward Multi-Relaying Systems

JUNQIAN ZHANG[1,2] AND HARRY LEIB[1]

[1] Department of Electrical and Computer Engineering, McGill University, Montreal, QC H3A 0E9, Canada
[2] Analog Devices, Inc., Toronto, ON M5G 2C8, Canada

CORRESPONDING AUTHOR: HARRY LEIB (e-mail: harry.leib@mcgill.ca)

ABSTRACT This article considers regularized Weighted Decision Feedback Differential Coherent (WDFDC) receivers for selective Detect-and-Forward multi-relaying systems, operating over fast fading channels. Non-regularized WDFDC receivers have been employed in such One-Way Relay Network (OWRN) with DQPSK modulation, and shown to provide significant performance gains over Conventional Differential Detection (CDD). This paper demonstrates, however, that such non-regularized WDFDC receivers are plagued by a BER increase phenomenon in the high SNR range due to decision feedback error propagation and intermittent transmissions from relays. Because of this effect, the non-regularized WDFDC receivers are unable to provide very low error rates, making them unsuitable for ultra-reliable communication systems. To address this problem, our paper introduces a novel WDFDC receiver based on a regularized linear predictor (RLP) for relay to destination channels. We show that such regularized WDFDC receivers yield significant performance gains over their non-regularized counterparts in the high SNR range, without noticeable degradation at low SNR. Regularized WDFDC receivers on relay to destination links enable OWRN systems to provide very low error rates, making them suitable for ultra-reliable communication over fast fading channels.

INDEX TERMS Cooperative communication, differential detection, noncoherent detection, regularization, relaying.

I. INTRODUCTION

Cooperative communication techniques have drawn significant interest in wireless networks research [1]–[5]. Cooperative communication allows single-antenna nodes to create a virtual multi-antenna system, where multiple signal realizations are received through independent fading channels. This communication technique provides potential benefits including system throughput improvement, interference mitigation and seamless service provision [6]. One of the earliest works on relay assisted cooperative communication is [7]. Amplify-and-Forward (AF) and Decode-and-Forward (DF) constitute two basic relaying protocols [5], [8]. In AF relaying, the received signal is forwarded to the destination after being amplified by relay nodes. With AF, noise accumulates with each re-transmission. In symbol oriented DF relaying, the received symbol is detected at the relay before being forwarded to the destination. In Selective Relaying (SR) [8]–[10], the relay forwards only a correctly detected symbol, otherwise it remains silent.

Most of the previous works [8]–[12] assume perfect knowledge of Channel State Information (CSI) at the destination. However, perfect CSI is difficult to obtain in practice, especially in fast fading environments. Differential modulation, allowing noncoherent or differentially coherent detection, provides a feasible solution not requiring CSI [4]. In [13], differential single-relay systems employing a selective DF protocol were considered for fading channels and extended to muti-relay systems in [14]. However, only a Conventional Differential Detector (CDD) was considered in [13], [14]. Differentially coherent detection techniques have been also considered in [15] for IEEE 802.15.4 wireless sensors networks, because of their low complexity. Triggered by future applications of IEEE 802.15.4, such as in machine-to-machine communication, which require ulra-reliable performance,

improved differentially coherent detection techniques capable of providing very low error rates with low complexity emerged to be of considerable interest.

While commonly used in practice, the performance of CDD is limited by an error floor when the normalized Doppler frequency is above a certain level [16]. This issue is addressed by Multiple-Symbol Detection (MSD) and Decision-Feedback Differential Coherent (DFDC) detection techniques where multiple received samples are used for detection. The MSD for MDPSK signals over AWGN channels of [17] has been extended to fading channels in [18]. The major disadvantage of MSD is its high computational complexity. The Decision-Feedback Differential Coherent (DFDC) detector for AWGN channels of [19], exploiting feedback from previously decoded symbols, was extended to fading channels in [20], [21]. The DFDC detector has a lower complexity [4] and reduces the error floor over fast fading channels [20]. The linear-prediction DFDC receiver of [21] has the additional benefit of maintaining good performance in the presence of frequency offsets. The DFDC receiver was also considered for differential quadrature amplitude modulation (DQAM) [22]. In [23], iterative decoding techniques based on DFDC detection were applied to massive MIMO system. Iterative DFDC detection was considered in [24] for convolutionaly coded DMPSK transmission over fading Rayleigh channels, and shown to achieve remarkable power efficiency gains over CDD. The advantages of DFDC detection motivated its application also in cooperative communication systems. In [25], a DFDC detector was considered for a Two-Way Relay Network (TWRN) employing a single-relay AF protocol. Weighted-DFDC (WDFDC) receivers were employed in selective DF multi-relay systems [16], and shown that over fast fading channels they provide significant performance gains over CDD.

In this work, we consider a selective symbol based DF (also termed Detect-and-Forward) multi-relay system with WDFDC receivers and threshold discrimination at the destination, over fast fading channels. Each relay node forwards only correctly detected symbols. Hold-and-combine (HC) WDFDC receivers, proposed in [16], are employed over relay-destination (RD) links. In [16], the simulated BER performance is considered only for P/N_0 values of up to 48 dB (where P is total transmission power in the system). In our work we demonstrate a BER increase phenomenon in such systems when P/N_0 is above 56 dB due to decision feedback error propagation and intermittent transmission over RD channels. This phenomenon does not allow to achieve very low error rates. Although increasing the number of relays can decrease the lowest achievable error rate, it is desirable from a complexity point of view to have a receiver that inherently does not exhibit such an effect. In this paper we analyze in depth the error propagation phenomenon that limits the performance of WDFDC receivers in multi-relay selective DF networks, and provide a model for its effect. Then, using the insight provided by such analysis we derive a novel WDFDC receiver based on a *regularized* linear predictor (RLP) that

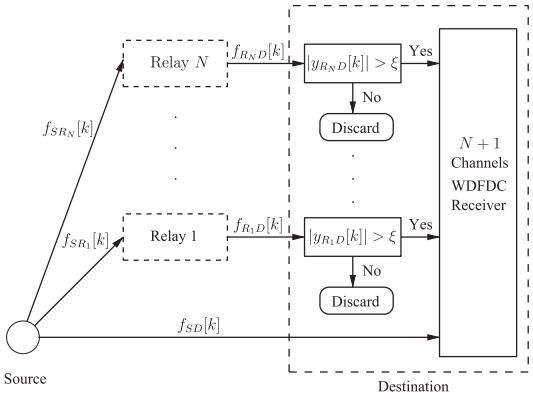

FIGURE 1. System model of a multiple relay OWRN.

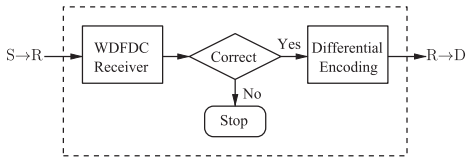

FIGURE 2. Relay node model.

is designed to reduce the effect of decision feedback errors and intermittent transmissions. Analysis results show a performance improvement for a wide range of frame sizes, that is more significant at low BER values where decision feedback errors dominate. Hence OWRN systems with regularized WDFDC receivers are attractive for applications demanding ultra-reliable services, such as machine-to-machine communication [2] [26], factory automation [27], and Common Public radio Interface (CPRI) systems [28].

The remainder of this paper is organized as follows. The model for selective DF multi-relay systems with WDFDC receivers, and the effect of decision feedback errors on single-relay systems are considered in Section II. Regularized WDFDC receivers are introduced in Section III. Multi-relay systems with non-regularized and regularized WDFDC receivers on RD links are considered in Section IV, and the conclusions are presented in Section V. Appendices A and B present a simple model for decision feedback error effects on performance, and the derivation of analytical performance bounds.

II. DETECT-AND-FORWARD MULTI-RELAYING SYSTEMS WITH WDFDC RECEIVERS

A. SYSTEM MODEL

Consider a one-way relay network (OWRN) where the transmission from the source to the destination is assisted by multiple relays as in [16], that we summarize for readers' convenience. Our system model is illustrated in Fig. 1, and similarly to [16] it consists of one source S, one destination D and N relays R_i, $i \in \{1, 2, \ldots, N\}$, with the relay model given in Fig. 2. Each relay has only one antenna, it cannot transmit and receive simultaneously, and hence it employs

a time division relaying protocol using $N+1$ phases. The source broadcasts its signal to all relays and destination in the first phase, and then each relay consumes one phase to forward the data to the destination if a correct symbol was detected, remaining silent otherwise. The destination employs a threshold ξ to allow only signals from active relays to be combined with the one from the source for detection purposes.

This work assumes differential QPSK with Gray mapping and WDFDC receivers. We assume ideal symbol synchronization, and all signals represented by their complex baseband equivalents. A QPSK symbol is denoted as $a[\cdot] \in \mathcal{A}_\phi = \{e^{j(\pi\nu/2)} | \nu \in \{0, 1, 2, 3\}\}$ and the corresponding differentially encoded symbol $b[k]$ is

$$b[k] = a[k]b[k-1], \qquad k \in \mathbb{Z} \tag{1}$$

where k is the symbol index. We assume the transmitter filter $H_T(f)$ and receiver filter $H_R(f)$ are square-root Nyquist. Therefore, there is no intersymbol interference as long as the continuous-time fading process $f_c(t)$, with equivalent single-sided bandwidth B_f, does not vary significantly during one symbol interval T [21]. We assume that these conditions are satisfied for normalized maximum Doppler frequency $B_f T \leq 0.05$. Then, the received signal sample can be written as

$$y[k] = y(kT) = \sqrt{P_0} f[k] b[k] + n[k] \tag{2}$$

where P_0 is the power allocation over the channel. The fading process $f[\cdot]$ is assumed correlated zero-mean complex Gaussian with normalized power $E\{|f[k]|^2\} = 1$, and the noise process $n[\cdot]$ is uncorrelated zero-mean complex Gaussian with variance $\sigma_n^2 = N_0$, where N_0 is the one-sided power spectral density of the underlying passband noise. We further assume all channels experience frequency non-selective Rayleigh fading following Jake's model. Furthermore, $f[\cdot]$ and $n[\cdot]$ are uncorrelated and independent for different channels. At the destination, the estimated symbol $\hat{a}[k]$ is determined by a multi-channel WDFDC receiver.

The version of the WDFDC receiver we consider is the same as the prediction-based DF-DD of [21, Fig.2]. The memory of the WDFDC receiver is of size L and it employs Pilot Initialization (PI) as in [16], where L pilot symbols are transmitted at the beginning of the frame allowing to start operation with error free fully loaded memory. The decoded symbol can be expressed as

$$\hat{a}[k] = \underset{\tilde{a}[k] \in \mathcal{A}_\phi}{\operatorname{argmax}} \{\mathrm{Re}\{\tilde{a}[k] g^*[k]\}\} \tag{3}$$

where the decision variable $g[k] = y[k]\hat{y}^*[k]$ is formed with the estimated reference

$$\hat{y}[k] = \sum_{\nu=1}^{L} p_\nu \prod_{\mu=1}^{\nu-1} \hat{a}[k-\mu] y[k-\nu], \tag{4}$$

and $\hat{a}[k-\nu]$, $1 \leq \nu \leq L-1$ are previous detected (or pilot) symbols. The feedback coefficients p_ν, $1 \leq \nu \leq L$, minimize the mean-square error (MSE) [21]

$$\begin{aligned} \sigma_{mse}^2 &= E\left\{|y[k] - a[k]\hat{y}[k]|^2\right\} \\ &= E\left\{\left| c[k] - \sum_{\nu=1}^{L} p_\nu c[k-\nu] \right|^2 \right\} \end{aligned} \tag{5}$$

where $c[k] \triangleq \sqrt{P} f[k] + n[k]/b[k]$, and can be obtained by solving the Yule-Walker equations [29]

$$\boldsymbol{\Phi}_c \mathbf{p}^* = \boldsymbol{\varphi_c} \tag{6}$$

with autocorrelation matrix (ACM) of $c[\cdot]$ defined as

$$\boldsymbol{\Phi}_c = \begin{bmatrix} R_c[0] & R_c[1] & \cdots & R_c[L-1] \\ R_c^*[1] & R_c[0] & \cdots & R_c[L-2] \\ \vdots & \vdots & \ddots & \vdots \\ R_c^*[L-1] & R_c^*[L-2] & \cdots & R_c[0] \end{bmatrix} \tag{7}$$

where

$$R_c[\lambda] \triangleq E\{c[k]c^*[k-\lambda]\} = PR_f[\lambda] + N_0\delta[\lambda] \tag{8}$$

$$\boldsymbol{\varphi_c} \triangleq [R_c[-1] \quad R_c[-2] \quad \cdots \quad R_c[-L]]^T \tag{9}$$

$$\mathbf{p} \triangleq [p_1 \quad p_2 \quad \cdots \quad p_L]^T. \tag{10}$$

In (8), $R_f[\lambda]$ is the autocorrelation function (ACF) of the fading process $f[\cdot]$, and $\delta[\cdot]$ is the discrete delta function. For Rayleigh fading following the Jake's model, we have $R_f[\lambda] = J_0(2\pi B_f T \lambda)$.

The OWRN system of Fig. 1 employs $N+1$ transmission phases. In the first phase, the source broadcasts $b_S[k] = a_S[k]b_S[k-1]$ to the destination and all relays. The corresponding received signals at the destination and each relay R_i, $i \in \{1, 2, \ldots, N\}$ are

$$\begin{aligned} y_{SD}[k] &= \sqrt{P_S} f_{SD}[k] b_S[k] + n_{SD}[k], \\ y_{SR_i}[k] &= \sqrt{P_S} f_{SR_i}[k] b_S[k] + n_{SR_i}[k] \end{aligned} \tag{11}$$

where P_S is the power allocated to the source. Then WDFDC detection is performed at each relay and the decoded symbols for $i \in \{1, 2, \ldots, N\}$ are

$$\begin{aligned} \hat{a}_{SR_i}[k] &= \underset{\tilde{a}_{SR_i}[k] \in \mathcal{A}_\phi}{\operatorname{argmax}} \{\mathrm{Re}\{\tilde{a}_{SR_i}[k] g_{SR_i}^*[k]\}\} \\ g_{SR_i}[k] &= y_{SR_i}[k]\hat{y}_{SR_i}^*[k], \\ \hat{y}_{SR_i}[k] &= \sum_{\nu=1}^{L} p_\nu \prod_{\mu=1}^{\nu-1} \hat{a}_{SR_i}[k-\mu] y_{SR_i}[k-\nu]. \end{aligned} \tag{12}$$

During the second to the $(N+1)$-th phase, each relay R_i, assigned to one phase, decides if it forwards or not. We assume an ideal relay which knows if the decoded information is correct or not. In practice, this situation can be approached by several methods. Detection with erasure is used in [30] to decide when the relay forwards. If the decision variable belongs to an erasure region, the relay remains silent. In [31],

the SNR of the received sample is compared to a threshold, and if the threshold is passed the sample is considered reliable with low probability of making a decoding error. In [32] the Instantaneous Bit Error Probability (IBEP) is computed and compared to a threshold at each relay. The relay forwards only if all the IBEPs in one frame pass the threshold. With an ideal relay, if $\hat{a}_{SR_i}[k] = a_S[k]$, the i-th relay R_i differentially encodes the decoded symbol and forwards it to the destination in the $(i+1)$-th phase. Otherwise, it remains silent. Therefore, the transmission from each relay to the destination can be intermittent and the previous transmission time at each relay can be any instant before the current time k. For R_i, we denote by $m_i(k)$ the last instant before k this relay detected correctly. Similarly, we define $m_i(m_i(k))$ as the latest time before instant $m_i(k)$ relay R_i detected correctly. For any k, all the instants before k when R_i detected correctly are: $m_i(k), m_i(m_i(k)), m_i(m_i(m_i(k))), \ldots$. A convenient notation for $m_i(k)$ nested j times is $m_i(k)_j$. We define $m_i(k)_0 = k$, and for any non-negative integers l, q we have $m_i(m_i(k)_l)_q = m_i(k)_{l+q}$. Hence the differentially encoded relay symbol can be expressed as $b_{R_i}[k] = a_S[k] b_{R_i}[m_i(k)_1]$.

We assume equal power allocation, $P_S = P_{R_1} = \cdots = P_{R_N} = P/(N+1)$, where P is the total transmitted power (the sum of transmitted power at all nodes). Then the received signal at the destination from relay R_i is

$$y_{R_iD}[k] = \begin{cases} \sqrt{P_{R_i}} f_{R_iD}[k] b_{R_i}[k] + n_{R_iD}[k], & \hat{a}_{SR_i}[k] = a_S[k] \\ n_{R_iD}[k], & \text{otherwise} \end{cases} \tag{13}$$

The destination employs thresholds ξ to allow only actual transmissions from R_i to be combined with the signal from the source and other relays. If $|y_{R_iD}[k]| > \xi$, then the signal is used in combining. We denote by $\hat{m}_i(k)$ the last instant before k when the received signal at destination from relay R_i passed the threshold. It is convenient to define $\hat{m}_i(k)_j$ as nesting of $\hat{m}_i(k)$ similarly as $m_i(k)_j$ with respect to $m_i(k)$. However because of noise and fading $\hat{m}_i(k)$ can be different from $m_i(k)$. The reference calculated by the WDFDC receiver for the R_iD channel is

$$\hat{y}_{R_iD}[k] = \sum_{\nu=1}^{L} p_\nu \prod_{\mu=1}^{\nu-1} \hat{a}_D[\hat{m}_i(k)_\mu] y_{R_iD}[\hat{m}_i(k)_\nu] \tag{14}$$

where p_ν are the feedback coefficients of the WDFDC receiver calculated by solving (6). This version of WDFDC receiver is denoted as Hold-and-Combine (HC) in [16], allowing p_ν to be calculated only once and to be the same for all SR_i and SD channels at a fixed SNR.

The decoded symbol at the destination is

$$\hat{a}_D[k] = \underset{\tilde{a}_D[k] \in \mathcal{A}_\phi}{\operatorname{argmax}} \{\operatorname{Re}\{\tilde{a}_D[k] (g_D^{DF}[k])^*\}\} \tag{15}$$

where the combined reference, assuming equal gain combining, is given by

$$g_D^{DF}[k] = y_{SD}[k] \hat{y}_{SD}^*[k] + \sum_{i=1}^{N} I_\xi[|y_{R_iD}[k]|] y_{R_iD}[k] \hat{y}_{R_iD}^*[k] \tag{16}$$

with

$$\hat{y}_{SD}[k] = \sum_{\nu=1}^{L} p_\nu \prod_{\mu=1}^{\nu-1} \hat{a}_D[k-\mu] y_{SD}[k-\nu] \tag{17}$$

$$I_\xi[|y_{R_iD}[k]|] = \begin{cases} 1, & \text{if } |y_{R_iD}[k]| > \xi \\ 0, & \text{otherwise.} \end{cases} \tag{18}$$

The effect of thresholding the received signals from relays at the destination in order to determine if a relay transmits or remains silent is encapsulated in (16), which represents a system with a variable number of diversity channels.

B. EFFECTS OF DECISION FEEDBACK ERRORS AND INTERMITTENT RELAY TRANSMISSIONS

In [16], the optimum feedback coefficients p_ν are obtained by assuming no decision feedback errors $\hat{a}[k-\nu] = a[k-\nu]$. In a realistic WDFDC receiver, that is impaired by decision feedback errors, the effective coefficients are different from the calculated optimum ones. The decision feedback symbols $\hat{a}[k-\mu]$, $1 \le \mu \le L-1$ can be expressed as

$$\hat{a}[k-\mu] \triangleq e^{j\hat{\varphi}[k-\mu]} = e^{j(\varphi[k-\mu] + \varphi_e[k-\mu])} \tag{19}$$

where $\varphi[\cdot]$ is the phase of the correct symbol $a[\cdot]$, and $\varphi_e[\cdot]$ is the phase error after a decision of the decoded symbol $\hat{a}[\cdot]$. With DQPSK we have $\varphi_e[\cdot] \in \mathcal{A}_e = \{0, \pi/2, -\pi/2, \pi\}$. Then the reference of the WDFDC receiver in (4) becomes

$$\begin{aligned} \hat{y}[k] &= \sum_{\nu=1}^{L} p_\nu \prod_{\mu=1}^{\nu-1} \hat{a}[k-\mu] y[k-\nu] \\ &= \sum_{\nu=1}^{L} p_\nu \prod_{\mu=1}^{\nu-1} e^{j(\varphi[k-\mu] + \varphi_e[k-\mu])} y[k-\nu] \\ &= \sum_{\nu=1}^{L} p'_\nu e^{j\sum_{\mu=1}^{\nu-1} \varphi[k-\mu]} y[k-\nu] \\ &= \sum_{\nu=1}^{L} p'_\nu \prod_{\mu=1}^{\nu-1} a[k-\mu] y[k-\nu] \end{aligned} \tag{20}$$

where

$$p'_\nu \triangleq p_\nu e^{j\sum_{\mu=1}^{\nu-1} \varphi_e[k-\mu]}, \qquad \nu = 1, 2, \ldots, L \tag{21}$$

are the effective feedback coefficients, that depend also on the phase errors $\varphi_e[k-\mu]$.

There is also an impairment induced by intermittent transmissions from relays. In (14) the feedback coefficients of the

WDFDC destination receiver are optimal only when its memory is loaded with successive received samples $y_{R_iD}[k-\nu]$. This can happen only when $\hat{m}_i(k)_\nu = k-\nu$, otherwise such coefficients p_ν are not optimal anymore. The effect on performance of such departure from optimality and the mismatch between p'_ν and p_ν due to decision feedback errors will be considered in the next section.

C. PERFORMANCE OF WDFDC RECEIVERS IN ONE RELAY SYSTEMS

In this section, we present simulation results for the performance of WDFDC receivers with PI in OWRN. All simulations were conducted over Rayleigh fading channels of $B_fT = 0.05$, using Jake's model IV from [33]. In this paper T is defined as one time slot that contains $N+1$ transmission phases. In all simulations, at least $5 \cdot 10^8$ information symbols were generated and the number of fading realizations varies based on the frame size of N_I symbols. The number of realizations is 10^7 when $N_I = 50$ and $5 \cdot 10^4$ when $N_I = 10^4$. The average BER is calculated when at least 500 bit errors are detected at each P/N_0 value, and the results are presented as a function of P/N_0, where $N_0 = 1$ for all channels. The BER for individual bits in a frame is calculated when at least 100 errors are accumulated for each data bit. Curves with Lower Bound (LB) labels (including Ideal Lower Bound (ILB), Ideal Tighter Lower Bound (ITLB) and Lower Bound with genie (LB, gen)) were generated assuming the destination knows when a relay transmits. Curves marked with "gen" correspond to a system with "genie" in all WDFDC receivers, where correct data symbols are fed to the memory avoiding decision feedback errors.

The BER performance with a single relay $N = 1$, employing WDFDC receivers with PI over *SR*, *SD* channels and an HC WDFDC receiver over *RD* channel is presented in Fig. 3. We see that at high P/N_0 the BER does not decrease monotonically with increasing P/N_0. At such high P/N_0 the system performance becomes dominated by the error propagation effect due to decision feedback errors since channel noise effects become less pronounced. In the low SNR range, the performance with small threshold ξ is a little better than with large ξ. As SNR increases, however, the performance improves when the threshold is increased. Inspecting the simulated LB, where the receiver knows when the relay transmits, shows that it is a little better than the results with a threshold for $P/N_0 \leq 40$ dB, but becomes very close to the results with $\xi = 3.5$ for larger values of P/N_0. Hence the threshold method works satisfactory. When in addition to knowing when the relay transmits, it also operates without decision feedback errors (by feeding the correct symbols into the memory of the WDFDC receivers), then we get the LB,gen curve in Fig. 3. Comparison of the LB and LB,gen curves in Fig. 3 shows that decision feedback errors significantly degrade performance. Comparing Fig. 3 and [16, Fig. 10], we see similar results for $\xi = 1$ and LB. However, [16, Fig. 10] only presents results for $P/N_0 \leq 40$ dB.

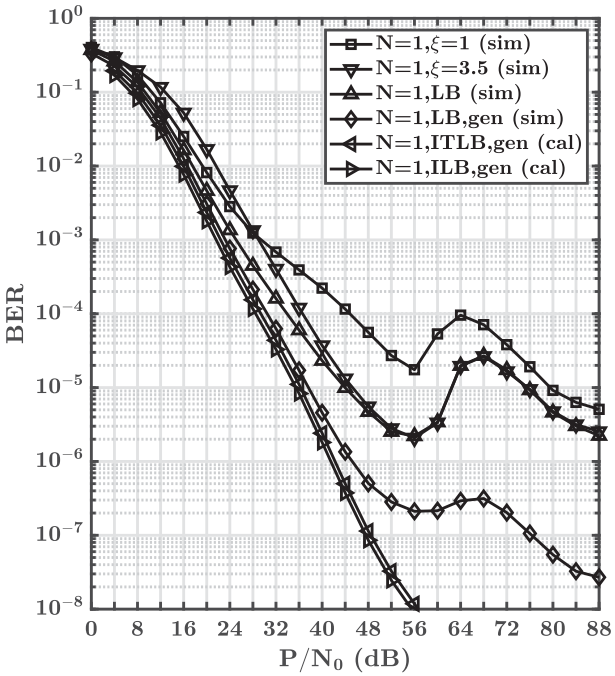

FIGURE 3. Simulated and Calculated BER for a OWRN with $N = 1$, employing WDFDC receiver with PI, $N_I = 50$, $L = 4$ and $B_fT = 0.05$.

An interesting phenomenon can be observed at $P/N_0 > 56$ dB, that when properly addressed can make multi-relay DF systems with WDFDC receivers achieve much lower BER than in [16], allowing their application in ultra-reliable communication systems such as in [26]–[28]. From Fig. 3 we observe that when $P/N_0 > 56$ dB, first the BER increases with P/N_0 and then it decreases for all ξ, as well as the LB. This behavior of the error rate was not found in [16]. To better understand this phenomenon we investigate the BER associated with individual bits in a frame, and present the results in Figs. 4–5. In Figs. 4 and 5 we present the results for $\xi = 1$ at low and high P/N_0 respectively. As we can see from Fig. 4 the first two bits in the frame perform the best, because with PI the first symbol is decoded with pilots loaded in the memory of the WDFDC receiver. As the bit index increases, decision errors are fed back to the memory and the performance deteriorates. When $P/N_0 < 56$ dB, as the bit index increases the performance becomes the same for all bits in Fig. 4. However, when $P/N_0 > 56$ dB the BER continues to increase with the bit index. In Fig. 5, the increase becomes linear in bit index, and this linearity behavior is maintained when $P/N_0 > 72$ dB. This behavior can be explained by the propagation of decision feedback errors. A model explaining this effect is presented in Appendix A. From Fig. 4, we can see that for $P/N_0 < 56$ dB, the BER stabilizes across the frame. For $P/N_0 \geq 56$ dB, the effect of error propagation becomes observable and eventually dominates the performance when $P/N_0 \geq 72$ dB in Fig. 5.

The effect of error propagation can be also seen in Fig. 6, where simulation results with a larger frame size $N_I = 10^4$ are

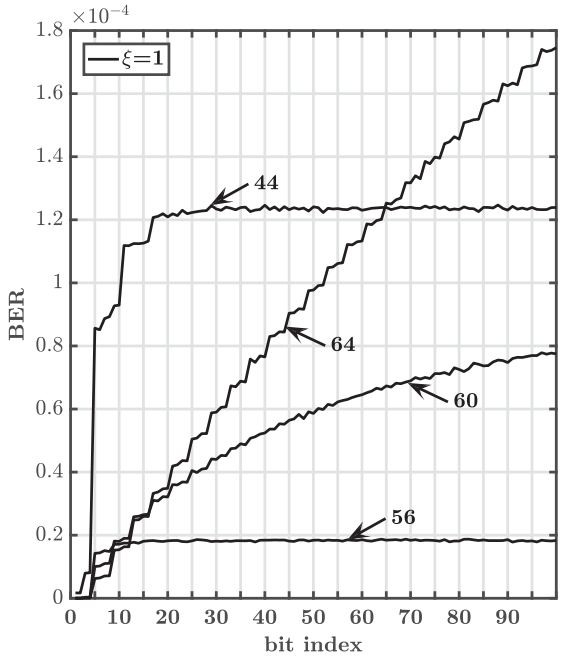

FIGURE 4. Simulated BER of individual bits in a frame of $N_I = 50$ at low P/N_0 (dB) for a OWRN with $N = 1$, $\xi = 1$, employing WDFDC receiver with PI, $L = 4$ and $B_fT = 0.05$.

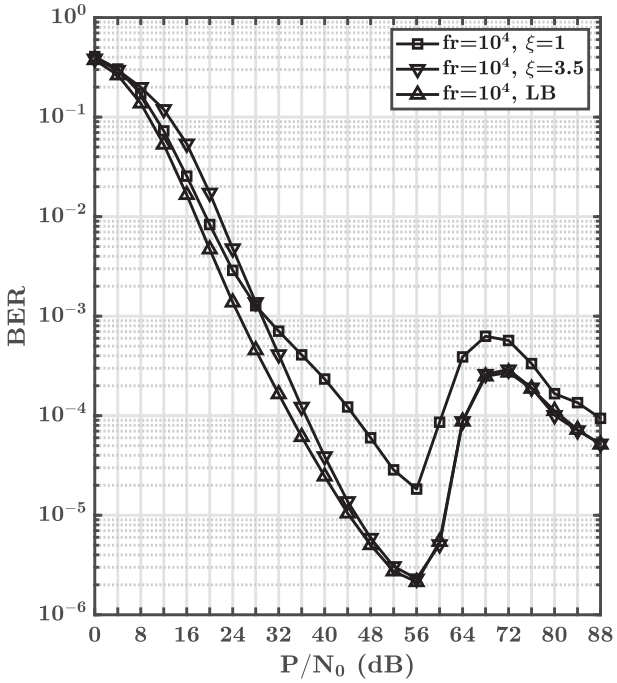

FIGURE 6. Simulated BER for a OWRN with $N = 1$, employing WDFDC receiver with PI, $N_I = 10^4$, $L = 4$ and $B_fT = 0.05$.

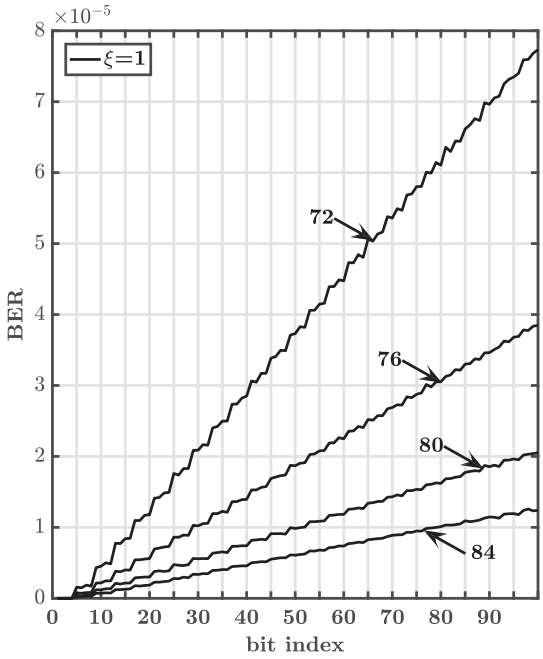

FIGURE 5. Simulated BER of individual bits in a frame of $N_I = 50$ at high P/N_0 (dB) for a OWRN with $N = 1$, $\xi = 1$, employing WDFDC receiver with PI, $L = 4$ and $B_fT = 0.05$.

presented. Comparison with Fig. 3 for $P/N_0 < 56$ dB shows almost the same performance for all ξ as well as the LB. For $P/N_0 \geq 56$ dB we see a more severe BER increase in Fig. 6 compared to Fig. 3. In this high P/N_0 region the effect of decision feedback errors propagation becomes more significant, and as the frame size increases more decision errors are accumulated resulting in an increase in the average BER over the frame.

Next, we discuss the analytical Ideal LB (ILB) and Ideal Tighter LB (ITLB) of Fig. 3, that are derived in Appendix B and presented in (59) (78) respectively. Both bounds assume a genie WDFDC receiver where the destination knows whether the relay transmits or not at each time instant. The ILB assumes that the relay receiver decodes correctly and hence transmits continuously, while the ITLB does not make this assumption and hence it transmits intermittently. The ITLB further assumes the memory of the WDFDC receiver is loaded with consecutive data samples, and hence the coefficients p_ν calculated by solving (6) are optimal. We can see from Fig. 3 that the ILB and ITLB are quite close. Compared to the ITLB in Fig. 3, the simulated LB,gen results, where the destination knows when a relay transmits however because of intermittent relay transmissions the memory of the WDFDC receivers is not necessary loaded with consecutive data samples, are similar in the low SNR range. As the SNR increases the difference between the ITLB and LB,gen curves become substantial revealing the BER increase phenomenon when $P/N_0 > 56$ dB. The simulated LB,gen curve indicates the loss induced by the departure from optimality of the coefficients p_ν calculated by (6) when the memory of the destination WDFDC receiver is loaded with nonconsecutive data samples because of intermittent transmissions from the relay. Comparison with the LB curve, where actual detected symbols are fed back, shows that the BER increase phenomenon occurs now at a much higher BER. In this case the BER cannot be lower, than $2 \cdot 10^{-6}$ for

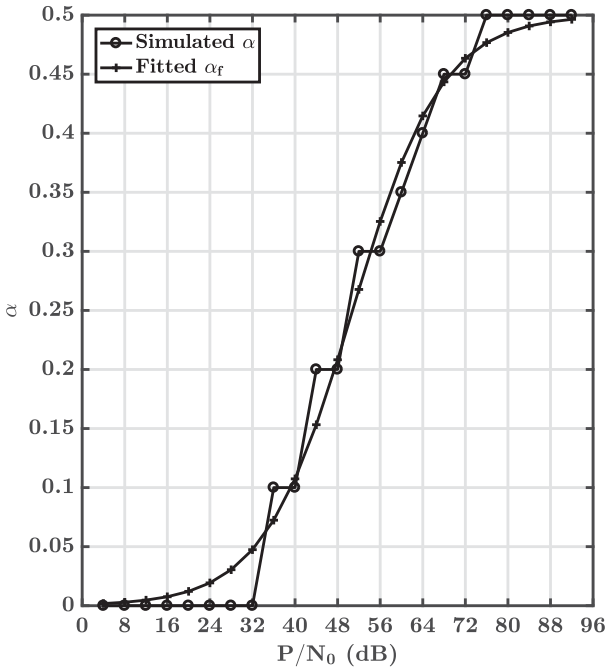

FIGURE 7. Simulated and fitted α_f of a OWRN with $N = 1$, employing regularized WDFDC receiver with PI, $N_I = 10^4$, $L = 4$ and $B_f T = 0.05$.

$P/N_0 \leq 88$ dB, showing the limitations of the non-regularized WDFDC receiver in providing very low error rates.

III. REGULARIZED WDFDC RECEIVERS

In this section, we introduce the regularized WDFDC receiver with PI for OWRN where the feedback coefficients are calculated using a Regularized Linear Predictor (RLP). Techniques based on RLP are studied in [34] to improve the spectral envelope estimate of speech by penalizing rapid changes. The performance of OWRN systems with non-regularized receivers suffers from the BER increase phenomenon due to decision feedback error propagation and intermittent transmissions on *RD* links, that cause a mismatch between the optimal and effective weights as discussed in Section II-B. To reduce the mismatch effects, we add the penalty function $\mathbf{p}^T\mathbf{X}\mathbf{p}^*$ to (5), where $\mathbf{p}$ is defined in (10) and $\mathbf{X}$ is the $L \times L$ matrix,

$$\mathbf{X} = \begin{bmatrix} \mathrm{SNR}_R^{\alpha} - 1 & 0 & \cdots & 0 \\ 0 & \mathrm{SNR}_R^{\alpha} - 1 & \cdots & 0 \\ \vdots & \vdots & \ddots & \vdots \\ 0 & 0 & \cdots & \mathrm{SNR}_R^{\alpha} - 1 \end{bmatrix}. \quad (22)$$

We assume $\mathrm{SNR}_R = (P/(N+1))/N_0 > 1$ which corresponds to practical operational conditions, and $\alpha > 0$ is the RLP parameter which determines the influence of SNR_R on the penalty function. We define the cost function for RLP as

$$C_R = \sigma_{mse}^2 + \mathbf{p}^T\mathbf{X}\mathbf{p}^*, \quad (23)$$

where σ_{mse}^2 is given in (5). Define $\mathbf{w} = \mathbf{p}^* = [p_1^* \quad p_2^* \cdots p_L^*]^T$ and $\mathbf{u} = [c[k-1] \quad c[k-2] \cdots c[k-L]]^T$. Then from (5) we have $\sigma_{mse}^2 = E\{|c[k] - \mathbf{w}^H\mathbf{u}|^2\}$ and (23) becomes

$$\begin{aligned} C_R &= E\{|c[k] - \mathbf{w}^H\mathbf{u}|^2\} + \mathbf{w}^H\mathbf{X}\mathbf{w} \\ &= E\{c[k]c^*[k]\} - \mathbf{w}^H E\{\mathbf{u}c^*[k]\} - E\{c[k]\mathbf{u}^H\}\mathbf{w} \\ &\quad + \mathbf{w}^H(E\{\mathbf{u}\mathbf{u}^H\} + \mathbf{X})\mathbf{w} \\ &= R_c[0] - \mathbf{w}^H\boldsymbol{\varphi_c} - \boldsymbol{\varphi_c}^H\mathbf{w} + \mathbf{w}^H(\boldsymbol{\Phi}_c + \mathbf{X})\mathbf{w} \end{aligned} \quad (24)$$

where we used (7), (8) and (9). It is easy to show that the RLP coefficients that minimize (24) are obtained by solving the equation

$$(\boldsymbol{\Phi}_c + \mathbf{X})\mathbf{p}^* = \boldsymbol{\varphi_c} \quad (25)$$

Note that when $\alpha = 0$, the penalty function is zero and (25) is equivalent to (6).

Next we determine the RLP parameter α. First, we consider a frame size of $N_I = 10^4$. For each P/N_0 value, we performed simulations with different α for the OWRN with $N = 1$ and the values of α that yield the lowest BER was entered in Fig. 7. Then using the simulated results, the parameter α is fitted to a logistic function

$$\alpha_f = \frac{0.5}{1 + e^{-z_2(SNR_{R,dB} - z_3)}} \quad (26)$$

where $SNR_{R,dB} = 10\log_{10}(\frac{\frac{P}{N+1}}{N_0})$, and z_2 z_3 represent the steepness and the midpoint of the curve. Using the Matlab nonlinear regression function "nlinfit" we found the fitted values $z_2 = 0.119878295501326$ and $z_3 = 47.802208775435666$.

The performance with regularized WDFDC receivers is investigated by using computer simulations as detailed in Section II-C. Results for the OWRN with $N = 1$, $N_I = 10^4$, employing non-regularized WDFDC receivers on *SR* and *SD* channels and regularized WDFDC receiver with fitted α_f on *RD* channel are presented in Fig. 8. Comparison with Fig. 6 shows that the regularized receiver significantly improves the performance at high P/N_0 and reduces the BER increase phenomenon. At the same time, no noticeable performance degradation is observed in the low P/N_0 range. Next we apply the fitted α_f for $N_I = 10^4$ to $N_I = 50$, and present the results in Fig. 9. Similar to our observation in the last section, at high P/N_0, a large ξ achieves lower BER and the performance converges to the LB as P/N_0 increases. Comparison with Fig. 3 shows that using a regularized WDFDC receiver eliminates the BER increase phenomenon and improves performance significantly for all ξ and the LB in the high P/N_0 range. The improvement becomes larger when the threshold increases. To provide more details, Fig. 10 presents the simulated BER of individual bits for $N = 1$ and $\xi = 1$. Comparison with Fig. 4 shows a better performance at $P/N_0 = 56$ dB when a regularized WDFDC receiver is used. Also, in Fig. 4, the BER starts to increase with the bit index at $P/N_0 = 60$ dB, and the increase becomes linear when $P/N_0 > 64$ dB However, in Fig. 10, the increase starts at $P/N_0 = 64$ dB with a

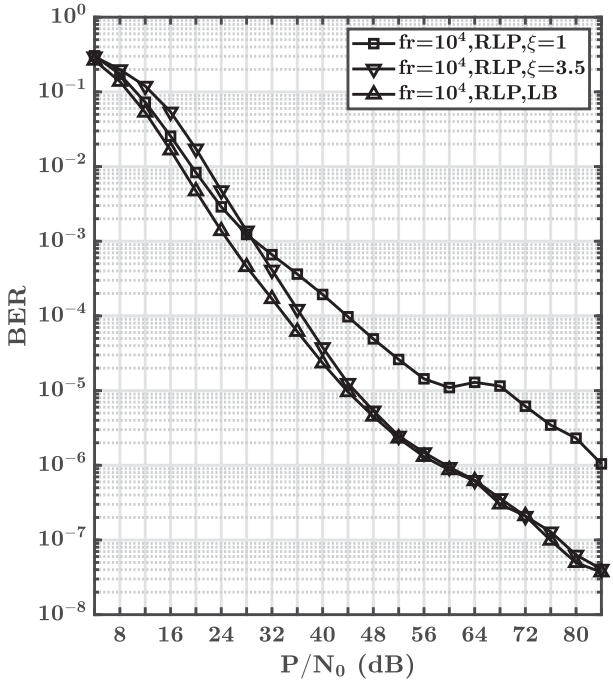

FIGURE 8. Simulated BER for a OWRN with $N = 1$, employing regularized WDFDC receivers with fitted α_f, PI, $N_I = 10^4$, $L = 4$ and $B_f T = 0.05$.

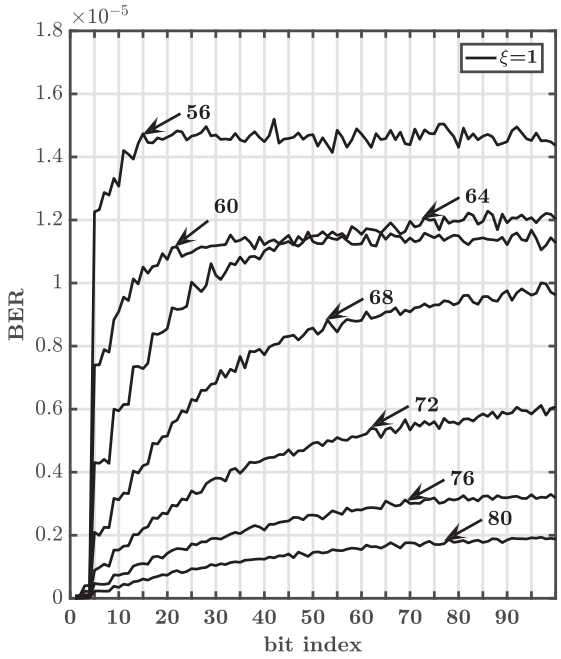

FIGURE 10. Simulated BER of individual bits in a frame of $N_I = 50$ at different P/N_0 (dB) for a OWRN with $N = 1$, $\xi = 1$, employing regularized WDFDC receiver with fitted α_f, PI, $N_I = 50$, $L = 4$ and $B_f T = 0.05$.

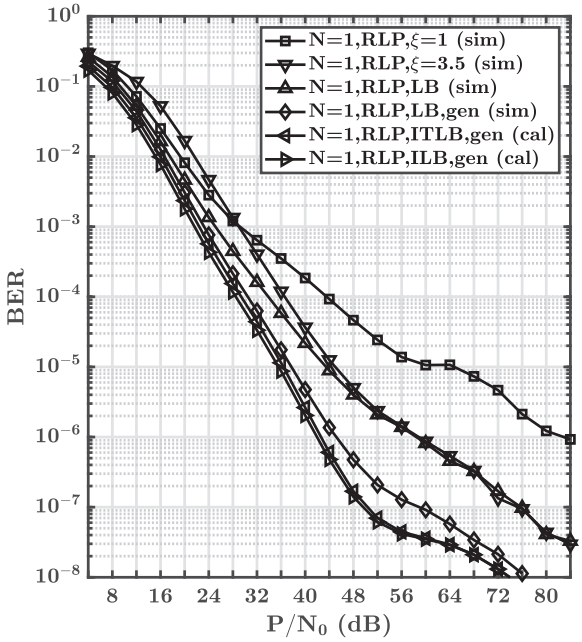

FIGURE 9. Simulated and calculated BER for a OWRN with $N = 1$, employing regularized WDFDC receiver with fitted α_f, PI, $N_I = 50$, $L = 4$ and $B_f T = 0.05$.

much smaller rate and the BER eventually saturates. Compared to Fig. 4, the linear BER increase with bit index is no longer observed in Fig. 10. We see that the use of regularized WDFDC receivers significantly reduces the error propagation effect at high P/N_0. The same conclusion can be also drawn by comparing results of different frame sizes, where the BER difference between Figs. 8 and 9 are much smaller than the one between Figs. 6 and 3 at high P/N_0.

We also present simulation results of the OWRN LB with genie regularized WDFDC receivers in Fig. 9. Compared to non-regularized receivers in Fig. 3, no BER increase is observed at high SNR. This shows that the use of regularized receivers reduces the mismatch effect of WDFDC weights caused by intermittent transmissions. This conclusion can also be reached by comparing the ITLB and the simulated LB with genie receivers, because the difference between the two curves is caused by the mismatch of WDFDC coefficients. In Fig. 9 we see that when regularized receivers are used, the difference becomes smaller than for non-regularized receivers in Fig. 3. Furthermore, the BER difference between the LB and the LB,gen with regularized receivers in Fig. 9 is lower than with non-regularized receivers of Fig. 3. This shows that also the error propagation effect on performance is reduced by the use of regularized WDFDC receivers on *RD* links.

The analytical ILB and ITLB with regularized WDFDC receivers are presented in Fig. 9. The ILB and ITLB derivations are presented in Appendix B and the curves correspond to (72) and (80) respectively. Compared to the ITLB in Fig. 3, when $P/N_0 < 48$ dB both curves show similar performance. However, when $P/N_0 \geq 48$ dB, the diversity order of the ILB and the ITLB in Fig. 9 decreases and both curves start to bend. This is because in the OWRN system with regularized receivers, the WDFDC receivers on *RD* and *SD* links employ different weights p_ν, resulting in two different singular points inside the contour integration used to evaluate these bounds,

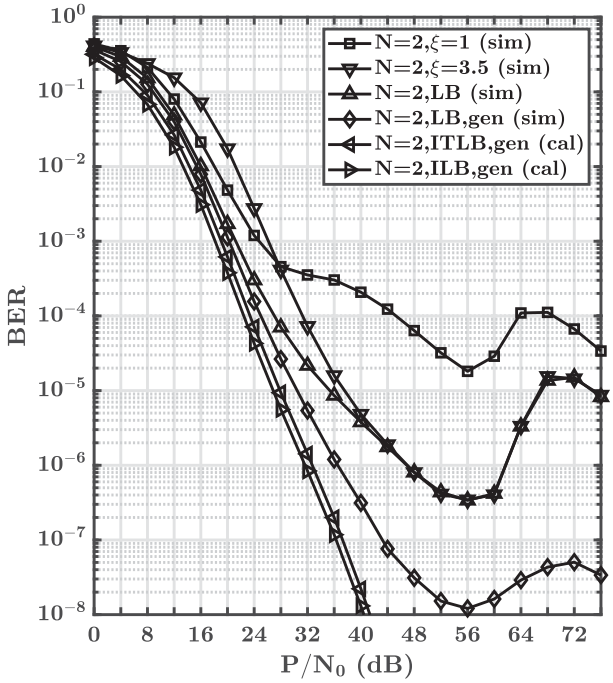

FIGURE 11. Simulated and calculated BER for a OWRN with $N = 2$, employing WDFDC receivers with PI, $N_I = 50$, $L = 4$ and $B_fT = 0.05$.

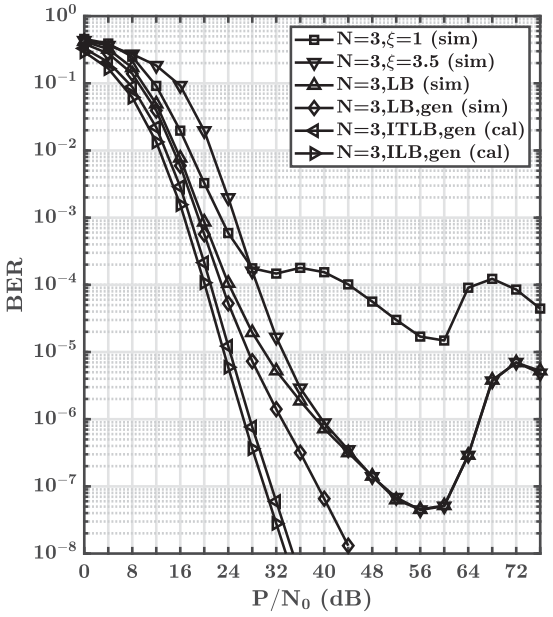

FIGURE 12. Simulated and calculated BER for a OWRN with $N = 3$, employing WDFDC receivers with PI, $N_I = 50$, $L = 4$ and $B_fT = 0.05$.

as shown in Appendix B. However, simulation results show that this analytical behavior at high values of P/N_0 is not observed in practice due to decision feedback errors and intermittent transmission on *RD* links that mask this effect.

IV. PERFORMANCE RESULTS FOR MULTI-RELAY SYSTEMS

In Figs. 11 and 12 we present the BER performance of OWRN with $N = 2$ and $N = 3$, employing WDFDC receivers with PI over *SR*, *SD* channels, and HC non-regularized WDFDC receivers over *RD* channels. Our simulation results are the same as the ones from [16, Figs. 14 and 15], where only the results for $P/N_0 \leq 48$ dB are presented and hence no BER increase phenomenon is observed. Similar to one relay results from Fig. 3, with multiple relays when P/N_0 increases a larger threshold provides better performance as illustrated in Figs. 11 and 12. With $N = 1$, the lowest BER of $2 \cdot 10^{-6}$ is observed at $P/N_0 = 56$ dB in Fig. 3. From Figs. 11 and 12 we see that at the same P/N_0, the BER reaches $3 \cdot 10^{-7}$ and $4 \cdot 10^{-8}$ when the number of relays increases to $N = 2$ and $N = 3$. Hence with non-regularized WDFDC receivers, the OWRN is able to achieve a considerable low BER when the number of relays increases. However, when $P/N_0 > 56$ dB, the BER increase phenomenon is observed in Figs. 11 and 12, and this increase becomes larger as N increases for high ξ as well as the LB. In this region, the error propagation effect becomes even more dominant when the number of relays increases. Also, Figs. 3, 11 and 12 show that the difference between the calculated ITLB and the simulated LB,gen receivers increases as N increases. This is because the intermittent transmissions between each relay and the destination become more dominant with increasing N.

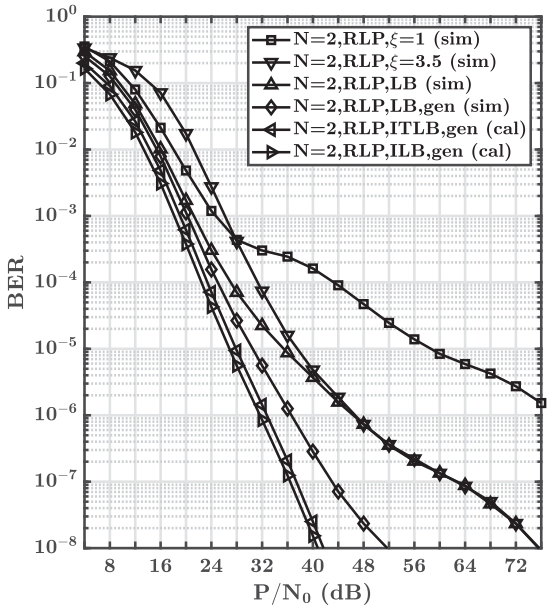

FIGURE 13. Simulated BER for a OWRN with $N = 2$, employing regularized WDFDC receivers with fitted α_f, PI, $N_I = 50$, $L = 4$ and $B_fT = 0.05$.

Simulation results of OWRN with regularized WDFDC receivers on *RD* links for $N = 2$ and $N = 3$ are presented in Figs. 13 and 14. Comparison of these figures with Figs. 11 and 12 shows that using regularized WDFDC receivers reduces the BER increase phenomenon and improves performance significantly for all thresholds in the high P/N_0 range when compared with the non-regularized counterparts.

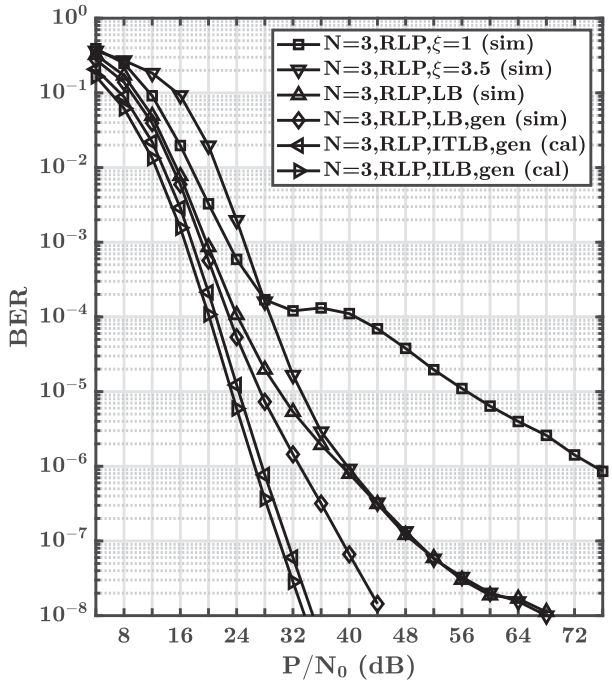

FIGURE 14. Simulated BER for a OWRN with $N = 3$, employing regularized WDFDC receivers with fitted α_f, PI, $N_I = 50$, $L = 4$ and $B_f T = 0.05$.

The improvement becomes more significant with increasing the number of relays. In the low P/N_0 region, systems with regularized receivers achieve the same performance as the non-regularized receivers for all N. For all N, regularized WDFDC receivers on *RD* links achieve a much lower BER when P/N_0 is increased than the non-regularized counterparts, without any degradation in the low P/N_0 range.

V. CONCLUSION

This paper considered selective detect-and-forward multi-relay systems with DQPSK modulation employing WDFDC receivers on *RD* links, and thresholds at the destination. When non-regularized WDFDC receivers are used on *RD* links, this paper shows the existence of a BER increase with SNR phenomenon in the high P/N_0 range. This phenomenon is caused by decision feedback error propagation and intermittent transmissions between relays and the destination. We introduced regularized WDFDC receivers, that are designed based on a regularized linear predictor for *RD* channels. This paper shows that such regularized receivers reduce the effects of decision feedback error and intermittent transmission, removing the BER increase phenomenon. The use of regularized WDFDC receivers yields significant performance gains over non-regularized counterparts in the high P/N_0 range without degradation at low P/N_0 values. The performance improvement is maintained for different frame sizes, and as the number of relays increases the improvement of regularized WDFDC receivers increases. This work shows that regularized WDFDC receivers in OWRN systems can provide very low BER, making such multi-relaying schemes attractive for ultra-reliable wireless communication systems such as in [26] [27] [28]. While this paper considered regularized WDFDC receivers for multi-relaying selective detect-and-forward schemes, other wireless communication systems could also benefit from such demodulation techniques not requiring carrier phase tracking.

APPENDIX A
A MODEL FOR ERROR PROPAGATION EFFECTS ON PERFORMANCE

Let E_k denote the error indicator for the k-th symbol in a frame. Then $E_k = 1$ implies that a symbol error occurred, and $E_k = 0$ means that the k-th symbol was detected correctly. The probability of the k-th symbol error is $\Pr[E_k = 1]$. We have

$$\Pr[E_k = 1] = \Pr[E_k = 1|E_{k-1} = 1]\Pr[E_{k-1} = 1] + \Pr[E_k = 1|E_{k-1} = 0]\Pr[E_{k-1} = 0] \quad (27)$$

Let $\Pr[E_k = 1|E_{k-1} = 1] = P_E(1|1)$ denote the error propagation factor. When $P_E(1|1)$ is close to one then we have a strong error propagation effect. Let $\Pr[E_k = 1|E_{k-1} = 0] = P_E(1|0)$ denote the symbol error probability when the previous symbol was decoded correctly. Also for convenience we use the notation $\Pr[E_k = 1] = P_{Ek}$. Then from (27)

$$P_{Ek} = (P_E(1|1) - P_E(1|0))P_{E(k-1)} + P_E(1|0)\,, \quad k = 0, 1, 2, \ldots \quad (28)$$

with $P_{E0} = 0$ corresponding to a pilot symbol. Notice that (28) represents a recursive equation for P_{Ek} where the key simplifying assumption is that $P_e(1|1)$ and $P_E(1|0)$ do not depend on k. We will see that despite such simplification, this model explains quite well the results we obtained from computer simulations.

The solution to (28) is

$$P_{Ek} = \frac{P_E(1|0)}{1 - (P_E(1|1) - P_E(1|0))}\cdot [1 - (P_E(1|1) - P_E(1|0))^k]\,,\ k = 0, 1, 2, \ldots \quad (29)$$

We have $P_{E1} = P_E(1|0)$ consistent with the fact that before the first information conveying symbol in the frame we have a pilot symbol and hence it can be considered as detected correctly with probability 1. When error propagation dominates then $P_E(1|1)$ is close to one. In general $P_E(1|0) << 1$. For the special case of $P_E(1|1) = 1$ then (29) is

$$P_{Ek} = 1 - (P_E(1|1) - P_E(1|0))^k \approx kP_E(1|0) \quad (30)$$

showing that P_{Ek} becomes linear in the symbol index k.

From (29) we have the probability of the n-th bit error for QPSK with Gray labeling given by

$$P_{en} = \frac{1}{2}P_{E\lceil \frac{n}{2} \rceil} = \frac{P_E(1|0)}{2 - 2(P_E(1|1) - P_E(1|0))}\cdot [1 - (P_E(1|1) - P_E(1|0))^{\lceil \frac{n}{2} \rceil}]\,,\ n = 0, 1, 2, \ldots, \quad (31)$$

where $\lceil \cdot \rceil$ denotes the ceiling operator. The n-th bit error probability of (31) is illustrated in Fig. 15 as a function of n

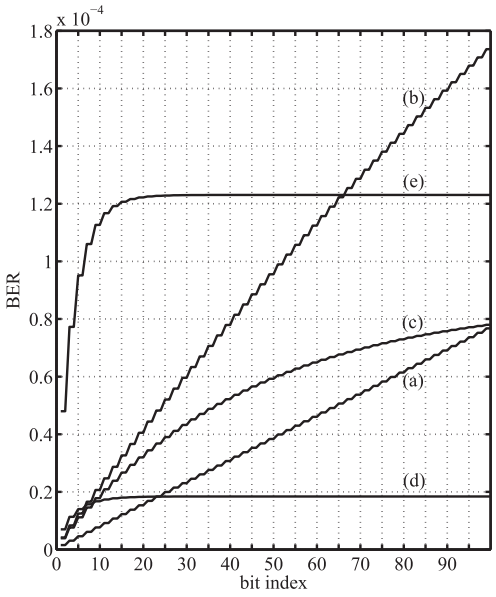

FIGURE 15. Calculated BER of individual bits using the model of Appendix A. (a) $P_E(1|1) = 1, P_E(1|0) = 3.07 \cdot 10^{-6}$. (b) $P_E(1|1) = 0.992, P_E(1|0) = 8.4 \cdot 10^{-6}$. (c) $P_E(1|1) = 0.995, P_E(1|0) = 7.8 \cdot 10^{-6}$. (d) $P_E(1|1) = 0.62, P_E(1|0) = 1.4 \cdot 10^{-5}$. (e) $P_E(1|1) = 0.61, P_E(1|0) = 9.6 \cdot 10^{-5}$.

for different values of $P_E(1|1)$ and $P_E(1|0)$. Curves (a) and (b) show the linear behavior of P_{en} with n when $P_E(1|1) \approx 1$, that is a manifestation of a strong error propagation phenomenon. Reducing a little $P_E(1|1)$ makes P_{en} to depart from being linear in n, as illustrated in curve (c) of Fig. 15. When $P_E(1|1)$ is more significantly less than one, then P_{en} becomes non-linear in n, and saturates as indicated by curves (d) and (e) of Fig. 15. Comparison of Fig. 15 with Figs. 4 and 5 shows that results obtained from (31) are in good agreement with corresponding simulation results.

APPENDIX B
DERIVATION OF ANALYTICAL BOUNDS
A. ILB OF A OWRN

We derive the analytical Ideal Lower Bound (ILB) for BER of an OWRN system with genie WDFDC receivers employing PI. The number of relays in the network is denoted as N and the size of the WDFDC receiver memory is denoted as L. We assume that each relay does not make errors and hence it transmits the correctly decoded symbols continuously. Therefore, at each time slot, the destination receives N transmissions from the relays and one from the source. The received signal at the destination over the m-th channel can be expressed as

$$y_m[k] = \sqrt{P_m} f_m[k] b_m[k] + n_m[k], \qquad m \in \{0, 1, \ldots, N\} \tag{32}$$

which corresponds to $SD, R_1D, \ldots, R_ND$ channels, and the differentially encoded information symbol is $b_m[k] = a[k]b_m[k-1]$. The decoded symbol at the destination is (15) and the combined decision signal $g_D^{DF}[k]$ in (16) becomes

$$g_D^{DF}[k] = \sum_{m=0}^{N} y_m[k]\hat{y}_m^*[k] \tag{33}$$

where $\hat{y}_m[k]$ is the reference calculated by m-th WDFDC receiver, assuming no decision feedback errors i.e. $\hat{a}_D[k-\mu] = a[k-\mu]$, and given by

$$\hat{y}_m[k] = \sum_{\nu=1}^{L} p_{\nu_m} \prod_{\mu=1}^{\nu-1} a[k-\mu] y_m[k-\nu]. \tag{34}$$

Since the BER for $\pi/4$-DQPSK and DQPSK are the same [21], for convenience we consider DQPSK in the analysis. The BER does not depend on the transmitted symbol, hence we assume $a[k] = e^{j\pi/4}$. Hence there is no decoding error if decision variable $g_D^{DF}[k]$ of (33) falls in the first quadrant. Denote by P_2, P_3 and P_4 the probability that $g_D^{DF}[k]$ falls into the second, third and fourth quadrant. With Gray mapping, one bit error occurs if $g_D^{DF}[k]$ lies in the second or fourth quadrant and two bit errors occur if it is in the third quadrant. Also, we have $P_2 = P_4$ because of symmetry. Then the BER is given by

$$\begin{aligned} P_b &= \frac{1}{2}(P_2 + P_4) + P_3 = P_2 + P_3 = \Pr\{\mathrm{Re}\{g_D^{DF}[k]\} < 0\} \\ &= \Pr\{D < 0\} = \int_{-\infty}^{0} p(D)dD \end{aligned} \tag{35}$$

$$D \triangleq g_D^{DF}[k] + g_D^{DF*}[k] = \sum_{m=0}^{N} (y_m[k]\hat{y}_m^*[k] + y_m^*[k]\hat{y}_m[k]). \tag{36}$$

Using the characteristic function $\phi_D(z)$, the BER can be expressed as [35] [36]

$$P_b = -\frac{1}{2\pi j} \int_{-j\infty-\epsilon}^{j\infty-\epsilon} \frac{\phi_D(z)}{z} dz \tag{37}$$

where $\phi_D(z)$ can be evaluated as in [37], since D can be expressed as a Hermitian quadratic form $D \triangleq \mathbf{v}^H \mathbf{Q} \mathbf{v}$ in Circular-Symmetric Complex Gaussian (CSCG) random variables. In our case, $\mathbf{v}$ and $\mathbf{Q}$ of size $2(N+1) \times 2(N+1)$ are given by

$$\mathbf{v} = \begin{bmatrix} y_0[k] & \hat{y}_0[k] & y_1[k] & \hat{y}_1[k] & \cdots & y_N[k] & \hat{y}_N[k] \end{bmatrix}^T \tag{38}$$

$$\mathbf{Q} = \mathrm{diag}(\mathbf{M}, \ldots, \mathbf{M}) \quad \text{where} \quad \mathbf{M} = \begin{bmatrix} 0 & 1 \\ 1 & 0 \end{bmatrix}. \tag{39}$$

Denote by $\bar{\mathbf{v}}$ and $\mathbf{L}$ the mean and covariance matrix of the vector $\mathbf{v}$. Then

$$\bar{\mathbf{v}} = \begin{bmatrix} E\{y_0[k]\} & E\{\hat{y}_0[k]\} & E\{y_1[k]\} & E\{\hat{y}_1[k]\} & \cdots \\ E\{y_N[k]\} & E\{\hat{y}_N[k]\} \end{bmatrix}^T.$$

With Rayleigh fading $E\{f_m[k]\} = 0$ and hence

$$E\{y_m[k]\} = E\{\sqrt{P_m} f_m[k] b_m[k] + n_m[k]\} = \sqrt{P_m} E\{f_m[k]\} E\{b_m[k]\} + E\{n_m[k]\} = 0 \quad (40)$$

$$E\{\hat{y}_m[k]\} = E\left\{\sum_{\nu=1}^{L} p_{\nu_m} \prod_{\mu=1}^{\nu-1} a[k-\mu] y_m[k-\nu]\right\} = \sum_{\nu=1}^{L} p_{\nu_m} \prod_{\mu=1}^{\nu-1} a[k-\mu] E\{y_m[k-\nu]\} = 0 \quad (41)$$

resulting in $\bar{\mathbf{v}} = \mathbf{0}$, and the covariance matrix is $\mathbf{L} = E\{\mathbf{v}\mathbf{v}^H\}$. Since the $N+1$ channels are independent we have $E\{y_m[k]y_n[k]^*\} = E\{\hat{y}_m[k]\hat{y}_n[k]^*\} = E\{y_m[k]\hat{y}_n[k]^*\} = 0$ where $m, n \in \{0, 1, \ldots, N\}$ and $m \neq n$, and hence

$$\mathbf{L} = \text{diag}(\mathbf{C}_0, \ldots, \mathbf{C}_N)$$

$$\mathbf{C}_m = \begin{bmatrix} E\{y_m[k]y_m[k]^*\} & E\{y_m[k]\hat{y}_m[k]^*\} \\ E\{\hat{y}_m[k]y_m[k]^*\} & E\{\hat{y}_m[k]\hat{y}_m[k]^*\} \end{bmatrix} = \begin{bmatrix} \mu_{mxx} & \mu_{mxy} \\ \mu_{mxy}^* & \mu_{myy} \end{bmatrix} \quad (42)$$

With equal power allocation, we have $P_m = P/(N+1)$, $m \in \{0, 1, \ldots, N\}$ and

$$\mu_{mxx} = \frac{P}{N+1} + N_0, \quad \mu_{mxy} = e^{j\pi/4} \frac{P}{N+1} \sum_{\nu=1}^{L} p_{\nu_m}^* R_f[\nu] \quad (43)$$

$$\mu_{myy} = \frac{P}{N+1} \sum_{\nu=1}^{L} \sum_{\mu=1}^{L} p_{\nu_m} p_{\mu_m}^* R_f[\mu-\nu] + N_0 \sum_{\nu=1}^{L} |p_{\nu_m}|^2 \quad (44)$$

Since $\bar{\mathbf{v}} = \mathbf{0}$, from [37] the characteristic function is

$$\phi_D(z) = \prod_{n=1}^{2N+2} \frac{1}{1 - z\lambda_n} \quad (45)$$

where λ_n are the eigenvalues of $\mathbf{LQ}$ of size $(2N+2) \times (2N+2)$. From (39) and (43), we have $\mathbf{LQ} = \text{diag}(\mathbf{C}_0\mathbf{M}, \ldots, \mathbf{C}_N\mathbf{M})$ showing that the eigenvalues of $\mathbf{LQ}$ are the eigenvalues of $\mathbf{C}_m\mathbf{M}$, $m \in \{0, 1, \ldots, N\}$. Denote the two eigenvalues of $\mathbf{C}_m\mathbf{M}$ as $\lambda_{1m}, \lambda_{2m}$, then for $q = 1, 2$

$$\lambda_{qm} = \frac{1}{2}\Big[(\mu_{mxy} + \mu_{mxy}^*) + (-1)^q \sqrt{(\mu_{mxy} + \mu_{mxy}^*)^2 + 4(\mu_{mxx}\mu_{myy} - |\mu_{mxy}|^2)}\Big] \quad (46)$$

From Cauchy–Schwarz inequality, we have $\mu_{mxx}\mu_{myy} > |\mu_{mxy}|^2$, hence $\lambda_{1m} < 0$ and $\lambda_{2m} > 0$.

Using (46) the characteristic function of (45) becomes

$$\phi_D(z) = \prod_{m=0}^{N} \frac{1}{(1 - z\lambda_{1m})(1 - z\lambda_{2m})} \quad (47)$$

and the BER in (37) can be expressed as

$$P_b = -\frac{1}{2\pi j} \int_{-j\infty-\epsilon}^{j\infty-\epsilon} \frac{\phi_D(z)}{z} dz = -\frac{1}{2\pi j} \int_{-j\infty-\epsilon}^{j\infty-\epsilon} \prod_{m=0}^{N} \frac{\lambda_{1m}^{-1}\lambda_{2m}^{-1}}{z(z - \lambda_{1m}^{-1})(z - \lambda_{2m}^{-1})} dz \quad (48)$$

In general, λ_{1m} and λ_{2m} are different for different channels $m \in \{0, 1, \ldots, N\}$ because each channel could employ different feedback weights p_{ν_m}, $\nu \in \{1, 2, \ldots, L\}$. Next, we consider two special cases of interest in this work. The first case considers OWRN systems with non-regularized WDFDC receivers where the same feedback weights are used for all channels. The second case considers the use of regularized WDFDC receivers on R_iD, $i \in \{1, 2, \ldots, N\}$ channels and a non-regularized WDFDC receiver on the SD channel. In both cases the BER is derived by using the Residue Theorem [38, p. 89].

1) OWRN WITH NON-REGULARIZED WDFDC RECEIVERS

In this case the WDFDC feedback coefficients p_ν, $\nu \in \{1, 2, \ldots, L\}$ are the same for all channels. Therefore, $\mathbf{C}_m$ of (43) are the same for all $m \in \{0, 1, \ldots, N\}$ and $\mathbf{LQ}$ has two eigenvalues λ_1 and λ_2 of order $N+1$ each. Then (47) becomes

$$\phi_D(z) = \frac{1}{(1 - z\lambda_1)^{N+1}(1 - z\lambda_2)^{N+1}}. \quad (49)$$

and the BER in (48) can be expressed as

$$P_b = -\frac{\lambda_1^{-N-1}\lambda_2^{-N-1}}{2\pi j} \int_{-j\infty-\epsilon}^{j\infty-\epsilon} \frac{1}{z(z - \lambda_1^{-1})^{N+1}(z - \lambda_2^{-1})^{N+1}} dz = -\frac{\lambda_1^{-N-1}\lambda_2^{-N-1}}{2\pi j} \int_{C_1} h_1(z) dz \quad (50)$$

where the anticlockwise oriented contour C_1 is closed to include the left-half plane, and exclude the pole at the origin by involving a small semi-circle detour around it. Since $\lambda_1 < 0$ and $\lambda_2 > 0$, the function $h_1(z)$ is analytic on and inside C_1 except for one singular point at pole λ_1^{-1}. According to the Residue Theorem [38, p. 89],

$$\int_{C_1} h_1(z) dz = 2\pi j \cdot \text{res}(h_1(z), z = \lambda_1^{-1}) \quad (51)$$

where the residue at λ_1^{-1} is given by [38, p. 90]

$$\text{res}(h_1(z), z = \lambda_1^{-1}) = \lim_{z \to \lambda_1^{-1}} \left\{\frac{1}{N!} \frac{d^N}{dz^N} \left[(z - \lambda_1^{-1})^{N+1} h_1(z)\right]\right\} = \lim_{z \to \lambda_1^{-1}} \left\{\frac{1}{N!} \frac{d^N}{dz^N} \frac{1}{z(z - \lambda_2^{-1})^{N+1}}\right\} = \lim_{z \to \lambda_1^{-1}} \left\{\frac{1}{N!} \frac{d^N}{dz^N} g_1(z)\right\} \quad (52)$$

In order to obtain the residue, we first calculate the N-th derivative of $g_1(z) \triangleq \frac{1}{z(z-\lambda_2^{-1})^{N+1}}$. Theorem 1 in [39] shows that $F^{(n)}(x)$, the n-th derivative of $F(x) = \prod_{i=1}^{m} f_i(x)$ with respect to x is

$$F^{(n)}(x) = n! \sum_{\substack{k_i \geq 0, i=1,2,\ldots,m \\ k_1+k_2+\cdots+k_m=n}} \prod_{q=1}^{m} \frac{f_q^{(k_q)}(x)}{k_q!} \tag{53}$$

where $f_q^{(k_q)}(x)$ is the k_qth derivative of $f_q(x)$. Define $g_1(z) \triangleq f_1(z)f_2(z)$ where $f_1(z) = \frac{1}{z}$, $f_2(z) = \frac{1}{(z-\lambda_2^{-1})^{N+1}}$. Then their k_1th and k_2th derivatives are $f_1^{(k_1)}(z) = (-1)^{k_1} k_1!\, z^{-k_1-1}$ and $f_2^{(k_2)}(z) = (-1)^{k_2} \frac{(N+k_2)!}{N!} (z-\lambda_2^{-1})^{-N-1-k_2}$. From (53), the N-th derivative of $g_1(z)$ becomes

$$\frac{d^N}{dz^N} g_1(z) = N! \sum_{\substack{k_1 \geq 0, k_2 \geq 0 \\ k_1+k_2=N}} \frac{f_1^{(k_1)}(z) f_2^{(k_2)}(z)}{k_1!\, k_2!} \tag{54}$$

and (52) becomes

$$\begin{aligned} \mathrm{res}(h_1(z), z = \lambda_1^{-1}) &= \lim_{z \to \lambda_1^{-1}} \left\{ \sum_{k_1+k_2=N} \frac{f_1^{(k_1)}(z) f_2^{(k_2)}(z)}{k_1!\, k_2!} \right\} \\ &= (-1)^N \sum_{k_2=0}^{N} \binom{N+k_2}{k_2} \lambda_1^{N-k_2+1} \left(\frac{\lambda_1 \lambda_2}{\lambda_2 - \lambda_1} \right)^{N+1+k_2} \end{aligned} \tag{55}$$

Then using (50), (51) and (55) we have

$$\begin{aligned} P_b &= -\lambda_1^{-N-1} \lambda_2^{-N-1} (-1)^N \cdot \\ &\quad \sum_{k_2=0}^{N} \binom{N+k_2}{k_2} \lambda_1^{N-k_2+1} \left(\frac{\lambda_1 \lambda_2}{\lambda_2 - \lambda_1} \right)^{N+1+k_2} \\ &= \frac{1}{(1-\lambda_2/\lambda_1)^{N+1}} \sum_{k_2=0}^{N} \binom{N+k_2}{k_2} \left(\frac{-\lambda_2/\lambda_1}{1-\lambda_2/\lambda_1} \right)^{k_2} \end{aligned} \tag{56}$$

Defining

$$v_{21} \triangleq -\lambda_2/\lambda_1 \tag{57}$$

(56) becomes

$$P_b = \frac{1}{(1+v_{21})^{N+1}} \sum_{k_2=0}^{N} \binom{N+k_2}{k_2} \left(\frac{v_{21}}{1+v_{21}} \right)^{k_2} \tag{58}$$

$$= \frac{1}{(1+v_{21})^{N+1}} \sum_{k_2=0}^{N} \binom{N+k_2}{k_2} \left(\frac{1}{1+1/v_{21}} \right)^{k_2} \tag{59}$$

Next, we rewrite (58) as

$$P_b = \frac{1}{(1+v_{21})^{2N+1}} \sum_{m=0}^{N} \binom{N+m}{m} v_{21}^m (1+v_{21})^{N-m}. \tag{60}$$

Using the Binomial Theorem $(1+v_{21})^{N-m} = \sum_{k=0}^{N-m} \binom{N-m}{k} v_{21}^k$ (60) becomes

$$P_b = \frac{1}{(1+v_{21})^{2N+1}} \sum_{m=0}^{N} \sum_{k=0}^{N-m} \binom{N+m}{m} \binom{N-m}{k} v_{21}^{m+k}. \tag{61}$$

Let $i = m + k$, then $k = i - m$ and we have

$$\begin{aligned} P_b &= \frac{1}{(1+v_{21})^{2N+1}} \sum_{m=0}^{N} \sum_{i=m}^{N} \binom{N+m}{m} \binom{N-m}{i-m} v_{21}^i \\ &= \frac{1}{(1+v_{21})^{2N+1}} \sum_{i=0}^{N} \sum_{m=0}^{i} \binom{N+m}{m} \binom{N-m}{i-m} v_{21}^i \end{aligned} \tag{62}$$

where we use the double finite summation property $\sum_{i=0}^{n} \sum_{j=0}^{i} a_{i,j} = \sum_{j=0}^{n} \sum_{i=j}^{n} a_{i,j}$ for the summation over the triangle $1 \leq j \leq i \leq n$. According to [40, p. 2] and [41, p. 7], we have

$$\begin{aligned} \sum_{m=0}^{i} \binom{N+m}{m} \binom{N-m}{i-m} &= \binom{N+m+N-m+1}{i} \\ &= \binom{2N+1}{i}. \end{aligned} \tag{63}$$

Therefore,

$$P_b = \frac{1}{(1+v_{21})^{2N+1}} \sum_{i=0}^{N} \binom{2N+1}{i} v_{21}^i \tag{64}$$

which is essentially the BER of OWRN with N relays derived in [16] using the method of [35]. Also, one can easily verify that v_{21} in [16] is equivalent to the one defined in (57).

2) OWRN WITH REGULARIZED WDFDC RECEIVERS

Assume regularized WDFDC receivers for R_iD channels and a non-regularized WDFDC receiver for the SD channel. We assume that the feedback weights of the N R_iD channels are the same, while the ones of the SD channel are different from those of the R_iD channels. Therefore, $\mathbf{C}_0$ and $\mathbf{C}_i$, $i > 0$ in (43) are different, resulting in $\mathbf{LQ}$ having 4 eigenvalues, $\lambda_{1S} < 0$ and $\lambda_{2S} > 0$ of order 1 and $\lambda_{1R} < 0$ and $\lambda_{2R} > 0$ of order N. Hence, the characteristic function in (47) becomes

$$\phi_D(z) = \frac{1}{(1-z\lambda_{1S})(1-z\lambda_{2S})(1-z\lambda_{1R})^N (1-z\lambda_{2R})^N}, \tag{65}$$

and the BER in (48) becomes

$$\begin{aligned} P_b &= -\frac{\lambda_{1S}^{-1} \lambda_{2S}^{-1} \lambda_{1R}^{-N} \lambda_{2R}^{-N}}{2\pi j} \cdot \\ &\quad \int_{-j\infty-\epsilon}^{j\infty-\epsilon} \frac{1}{z(z-\lambda_{1S}^{-1})(z-\lambda_{2S}^{-1})(z-\lambda_{1R}^{-1})^N (z-\lambda_{2R}^{-1})^N} dz \\ &\triangleq -\frac{\lambda_{1S}^{-1} \lambda_{2S}^{-1} \lambda_{1R}^{-N} \lambda_{2R}^{-N}}{2\pi j} \int_{C_2} h_2(z) dz \end{aligned} \tag{66}$$

where the anticlockwise oriented contour C_2 is closed to include the left-half plane, with the pole at the origin excluded by involving a small semi-circle detour around it. Then the function $h_2(z)$ is analytic on and inside the contour C_2 except for two singular points at λ_{1S}^{-1} and λ_{1R}^{-1}. According to the Residue Theorem [38, p. 89],

$$\int_{C_2} h_2(z)dz = 2\pi j \cdot \left(\text{res}(h_2(z), z=\lambda_{1S}^{-1}) + \text{res}(h_2(z), z=\lambda_{1R}^{-1})\right). \quad (67)$$

Since the pole λ_{1S}^{-1} has order 1, then

$$\text{res}(h_2(z), z=\lambda_{1S}^{-1}) = (z-\lambda_{1S}^{-1})h_2(z)|_{z=\lambda_{1S}^{-1}} = \frac{1}{\lambda_{1S}^{-1}(\lambda_{1S}^{-1}-\lambda_{2S}^{-1})(\lambda_{1S}^{-1}-\lambda_{1R}^{-1})^N(\lambda_{1S}^{-1}-\lambda_{2R}^{-1})^N}. \quad (68)$$

The pole λ_{1R}^{-1} has order N, then according to [38, p. 90]

$$\text{res}(h_2(z), z=\lambda_{1R}^{-1}) = \lim_{z\to\lambda_{1R}^{-1}} \left\{ \frac{1}{(N-1)!}\frac{d^{N-1}}{dz^{N-1}} g_2(z) \right\} \quad (69)$$

where $g_2(z) \triangleq f_1(z)f_2(z)f_3(z)f_4(z)$ with

$$f_1(z) = \frac{1}{z} \quad f_2(z) = \frac{1}{z-\lambda_{1S}^{-1}}$$
$$f_3(z) = \frac{1}{z-\lambda_{2S}^{-1}} \quad f_4(z) = \frac{1}{(z-\lambda_{2R}^{-1})^N} \quad (70)$$

Using (53), the N-1th derivative of $g_2(z)$ is

$$\frac{d^{N-1}}{dz^{N-1}} g_2(z) = (N-1)! \sum_{\substack{k_i\geq 0, i=1,2,3,4 \\ k_1+k_2+k_3+k_4=N-1}} \frac{1}{k_1!k_2!k_3!k_4!} \prod_{q=1}^{4} f_q^{(k_q)}(z)$$

where $f_t^{(k_t)}(z)$ can be found from (70)

$$f_1^{(k_1)}(z) = (-1)^{k_1}k_1!\, z^{-k_1-1}$$
$$f_2^{(k_2)}(z) = (-1)^{k_2}k_2!\,(z-\lambda_{1S}^{-1})^{-k_2-1}$$
$$f_3^{(k_3)}(z) = (-1)^{k_3}k_3!\,(z-\lambda_{2S}^{-1})^{-k_3-1}$$
$$f_4^{(k_4)}(z) = (-1)^{k_4}\frac{(N+k_4-1)!}{(N-1)!}(z-\lambda_{2R}^{-1})^{-N-k_4}.$$

Then the residue in (69) becomes

$$\begin{aligned}
&\text{res}(h_2(z), z=\lambda_{1R}^{-1}) \\
&= \lim_{z\to\lambda_{1R}^{-1}} \left\{ \sum_{\substack{k_i\geq 0, i=1,\ldots,4 \\ k_1+k_2+k_3+k_4=N-1}} \frac{1}{k_1!k_2!k_3!k_4!} \prod_{t=1}^{4} f_t^{(k_t)}(z) \right\} \\
&= \frac{(-1)^{N-1}\lambda_{1R}^N}{(\lambda_{1R}^{-1}-\lambda_{1S}^{-1})(\lambda_{1R}^{-1}-\lambda_{2S}^{-1})(\lambda_{1R}^{-1}-\lambda_{2R}^{-1})^N} \cdot \\
&\sum_{\substack{k_i\geq, i=2,3,4 \\ k_2+k_3+k_4\leq N-1}} \binom{N+k_4-1}{k_4} \left(1-\frac{\lambda_{1R}}{\lambda_{1S}}\right)^{-k_2} \\
&\times \left(1-\frac{\lambda_{1R}}{\lambda_{2S}}\right)^{-k_3} \left(1-\frac{\lambda_{1R}}{\lambda_{2R}}\right)^{-k_4} \quad (71)
\end{aligned}$$

Using (66), (67), (68) and (71) we have (72) on the bottom of the page.

B. ITLB OF AN OWRN SYSTEM

We derive an analytical Ideal Tighter Lower Bound (ITLB) for BER of an OWRN system. Since each relay forwards only a correctly decoded symbol to the destination, and remains silent if it decodes an error, not all relays are active at each time instant. Hence, we denote by n_a the number of active relays. We also assume the destination knows whether each relay transmits or not at each time instant. Furthermore, we assume genie WDFDC receivers meaning no decision feedback errors occur. In this case the BER at the destination can be expressed as

$$P_b = \sum_{n_a=0}^{N} P_{b|n_a} P_a(n_a) \quad (74)$$

$$\begin{aligned}
P_b =& -\lambda_{1S}^{-1}\lambda_{2S}^{-1}\lambda_{1R}^{-N}\lambda_{2R}^{-N}\left[\text{res}(h_2(z), z=\lambda_{1S}^{-1}) + \text{res}(h_2(z), z=\lambda_{1R}^{-1})\right] \\
=& \frac{1}{(1+v_{2S1S})(1+v_{1R1S})^N(1+v_{2R1S})^N} + \frac{1}{(1+v_{1S1R})(1+v_{2S1R})(1+v_{2R1R})^N} \\
&\cdot \sum_{\substack{k_2\geq 0}}\sum_{k_3\geq 0}\sum_{k_4\geq 0} \binom{N+k_4-1}{k_4} \left(\frac{1}{1+1/v_{2R1R}}\right)^{k_4} \left(\frac{1}{1+1/v_{2S1R}}\right)^{k_3} \left(\frac{1}{1+1/v_{1S1R}}\right)^{k_2} \quad (72) \\
&\quad k_2+k_3+k_4\leq N-1
\end{aligned}$$

where

$$v_{2S1S} \triangleq -\frac{\lambda_{2S}}{\lambda_{1S}},\ v_{1S1R} \triangleq -\frac{\lambda_{1S}}{\lambda_{1R}},\ v_{1R1S} \triangleq -\frac{\lambda_{1R}}{\lambda_{1S}},\ v_{2S1R} \triangleq -\frac{\lambda_{2S}}{\lambda_{1R}},\ v_{2R1S} \triangleq -\frac{\lambda_{2R}}{\lambda_{1S}},\ v_{2R1R} \triangleq -\frac{\lambda_{2R}}{\lambda_{1R}} \quad (73)$$

$$P_{b|n_a} = \frac{1}{(1+v_{2S1S})(1+v_{1R1S})^{n_a}(1+v_{2R1S})^{n_a}} + \frac{1}{(1+v_{1S1R})(1+v_{2S1R})(1+v_{2R1R})^{n_a}} \cdot \sum_{\substack{k_2\geq 0\, k_3\geq 0\, k_4\geq 0 \\ k_2+k_3+k_4\leq n_a-1}} \sum\sum\sum \binom{n_a+k_4-1}{k_4} \left(\frac{1}{1+1/v_{2R1R}}\right)^{k_4} \left(\frac{1}{1+1/v_{2S1R}}\right)^{k_3} \left(\frac{1}{1+1/v_{1S1R}}\right)^{k_2} \tag{79}$$

$$P_b = \frac{1}{(1+v_{2S1S})^N} \sum_{n_a=0}^{N} \left[\frac{1}{(1+v_{2S1S})(1+v_{1R1S})^{n_a}(1+v_{2R1S})^{n_a}} + \frac{1}{(1+v_{1S1R})(1+v_{2S1R})(1+v_{2R1R})^{n_a}} \cdot \sum_{\substack{k_2\geq 0\, k_3\geq 0\, k_4\geq 0 \\ k_2+k_3+k_4\leq n_a-1}} \sum\sum\sum \binom{n_a+k_4-1}{k_4} \left(\frac{1}{1+1/v_{2R1R}}\right)^{k_4} \left(\frac{1}{1+1/v_{2S1R}}\right)^{k_3} \left(\frac{1}{1+1/v_{1S1R}}\right)^{k_2} \right] \binom{N}{n_a} v_{2S1S}^{n_a} \tag{80}$$

where $P_a(n_a)$ is the probability that the number of active relays is n_a, and it can be expressed as

$$P_a(n_a) = \binom{N}{n_a} (1-P_{b,SR})^{n_a} P_{b,SR}^{N-n_a} \tag{75}$$

where $P_{b,SR} = 1/(1+v_{2S1S})$ is the BER of a single link non-regularized WDFDC receiver at the relay. Then (75) becomes

$$P_a(n_a) = \binom{N}{n_a} \left(\frac{v_{2S1S}}{1+v_{2S1S}}\right)^{n_a} \frac{1}{(1+v_{2S1S})^{N-n_a}} = \frac{1}{(1+v_{2S1S})^N} \binom{N}{n_a} v_{2S1S}^{n_a}. \tag{76}$$

In (74) $P_{b|n_a}$ denotes the conditional BER at the destination when the number of active relays is n_a. The following section considers two cases, OWRN with non-regularized WDFDC receivers, and with regularized WDFDC receivers on R_iD channels.

1) OWRN WITH NON-REGULARIZED WDFDC RECEIVERS

The SD and R_iD, $i \in \{1, 2, \ldots, N\}$ channels employ non-regularized WDFDC receivers. From (59) we have

$$P_{b|n_a} = \frac{1}{(1+v_{2S1S})^{n_a+1}} \sum_{k_2=0}^{n_a} \binom{n_a+k_2}{k_2} \left(\frac{1}{1+1/v_{2S1S}}\right)^{k_2} \tag{77}$$

since the parameter v_{21} in (57) is the same as v_{2S1S} in (73). Using (76) and (77) in (74) results in

$$P_b = \sum_{n_a=0}^{N} \frac{1}{(1+v_{2S1S})^{n_a+1}} \cdot \sum_{k_2=0}^{n_a} \binom{n_a+k_2}{k_2} \left(\frac{1}{1+1/v_{2S1S}}\right)^{k_2} \frac{1}{(1+v_{2S1S})^N} \binom{N}{n_a} v_{2S1S}^{n_a} = \sum_{n_a=0}^{N} \binom{N}{n_a} \frac{v_{2S1S}^{n_a}}{(1+v_{2S1S})^{N+n_a+1}} \sum_{k_2=0}^{n_a} \binom{n_a+k_2}{k_2} \times \left(\frac{1}{1+1/v_{2S1S}}\right)^{k_2} \tag{78}$$

2) OWRN WITH REGULARIZED WDFDC RECEIVERS

The SD channel employs a non-regularized receiver while the R_iD channels use regularized receivers. From (72), we have (79) on the top of this page. where the parameters are defined in (73) and $\sum_{x=a}^{b}(\cdot) = 0$ if $a > b$. Using (79) and (76) in (74) results in (80) on the top of this page.

REFERENCES

[1] H. V. Nguyen, S. X. Ng, W. Liang, P. Xiao, and L. Hanzo, "A network-coding aided road-map of large-scale near-capacity cooperative communication," *IEEE Access*, vol. 6, pp. 21 592–21 620, 2018.

[2] M. N. Tehrani, M. Uysal, and H. Yanikomeroglu, "Device-to-device communication in 5G cellular networks: Challenges, solutions, and future directions," *IEEE Commun. Mag.*, vol. 52, no. 5, pp. 86–92, May 2014.

[3] M. Peng, Y. Li, Z. Zhao, and C. Wang, "System architecture and key technologies for 5G heterogeneous cloud radio access networks," *IEEE Netw.*, vol. 29, no. 2, pp. 6–14, Mar. 2015.

[4] L. Li, H. V. Poor, and L. Hanzo, "Non-coherent successive relaying and cooperation: Principles, design, and applications," *IEEE Commun. Surv. Tut.*, vol. 17, no. 3, pp. 1708–1737, Jul.–Sep. 2015.

[5] E. Hossain, D. I. Kim, and V. K. Bhargava, *Cooperative Cellular Wireless Networks*. New York, NY, USA: Cambridge Univ. Press, 2011.

[6] W. Zhuang and M. Ismail, "Cooperation in wireless communication networks," *IEEE Wireless Commun.*, vol. 19, no. 2, pp. 10–20, Apr. 2012.

[7] E. C. Van Der Meulen, "Three-terminal communication channels," *Advances Appl. Probability*, vol. 3, no. 1, pp. 120–154, 1971.

[8] J. N. Laneman, D. N. C. Tse, and G. W. Wornell, "Cooperative diversity in wireless networks: Efficient protocols and outage behavior," *IEEE Trans. Inf. Theory*, vol. 50, no. 12, pp. 3062–3080, Dec. 2004.

[9] G. Farhadi and N. C. Beaulieu, "Selective decode-and-forward relaying scheme for multi-hop diversity transmission systems," in *Proc. IEEE Global Telecommun. Conf.*, Nov. 2007, pp. 4385–4390.

[10] W. Su, A. K. Sadek, and K. J. R. Liu, "SER performance analysis and optimum power allocation for decode-and-forward cooperation protocol in wireless networks," in *Proc. IEEE Wireless Commun. Netw. Conf.*, vol. 2, Mar. 2005, pp. 984–989.

[11] E. Liu, X. Wang, Z. Wu, S. Hao, and Y. Dong, "Outage analysis of decode-and-forward two-way relay selection with different coding and decoding schemes," *IEEE Syst. J.*, vol. 13, no. 1, pp. 125–136, Mar. 2019.

[12] H. Chen, J. Liu, C. Zhai, and Y. Liu, "Performance of incremental-selective decode-and-forward relaying cooperative communications over Rayleigh fading channels," in *Proc. Int. Conf. Wireless Commun. Signal Process.*, Nov. 2009, pp. 1–5.
[13] T. Himsoon, W. P. Siriwongpairat, W. Su, and K. J. R. Liu, "Differential modulation with threshold-based decision combining for cooperative communications," *IEEE Trans. Signal Process.*, vol. 55, no. 7, pp. 3905–3923, Jul. 2007.
[14] T. Himsoon, W. P. Siriwongpairat, W. Su, and K. J. R. Liu, "Differential modulations for multinode cooperative communications," *IEEE Trans. Signal Process.*, vol. 56, no. 7, pp. 2941–2956, Jul. 2008.
[15] G. Zhang, H. Wen, L. Wang, P. Xie, and L. Song, "Simple adaptive single differential coherence detection of BPSK signals in IEEE 802.15.4 wireless sensor networks," *Sensors (MDPI)*, vol. 18, no. 2, pp. 1–19, 2017, doi: 10.3390/s18010052.
[16] G. Dai and H. Leib, "Detect-and-forward multirelay systems with decision-feedback differential coherent receivers," *IEEE Trans. Wireless Commun.*, vol. 15, no. 2, pp. 1267–1281, Feb. 2016.
[17] D. Divsalar and M. K. Simon, "Multiple-symbol differential detection of MPSK," *IEEE Trans. Commun.*, vol. 38, no. 3, pp. 300–308, Mar. 1990.
[18] D. Divsalar and M. K. Simon, "Maximum-likelihood differential detection of uncoded and trellis coded amplitude phase modulation over AWGN and fading channels-metrics and performance," *IEEE Trans. Commun.*, vol. 42, no. 1, pp. 76–89, Jan. 1994.
[19] H. Leib and S. Pasupathy, "The phase of a vector perturbed by Gaussian noise and differentially coherent receivers," *IEEE Trans. Inf. Theory*, vol. 34, no. 6, pp. 1491–1501, Nov. 1988.
[20] R. Schober, W. H. Gerstacker, and J. B. Huber, "Decision-feedback differential detection of MDPSK for flat Rayleigh fading channels," *IEEE Trans. Commun.*, vol. 47, no. 7, pp. 1025–1035, Jul. 1999.
[21] R. Schober and W. H. Gerstacker, "Decision-feedback differential detection based on linear prediction for MDPSK signals transmitted over Ricean fading channels," *IEEE J. Sel. Areas Commun.*, vol. 18, no. 3, pp. 391–402, Mar. 2000.
[22] C. Xu, S. X. Ng, and L. Hanzo, "Multiple-symbol differential sphere detection and decision-feedback differential detection conceived for differential QAM," *IEEE Trans. Veh. Technol.*, vol. 65, no. 10, pp. 8345–8360, Oct. 2016.
[23] C. Stierstorfer, R. F. H. Fischer, and G. Yammine, "Iterative decision-feedback in non-coherent multi-user massive MIMO systems," in *Proc. WSA 19th Int. ITG Workshop Smart Antennas*, Mar. 2015, pp. 1–8.
[24] L. H. J. Lampe and R. Schober, "Iterative decision-feedback differential demodulation of bit-interleaved coded MDPSK for flat Rayleigh fading channels," *IEEE Trans. Commun.*, vol. 49, no. 7, pp. 1176–1184, Jul. 2001.
[25] T. Cui, F. Gao, and C. Tellambura, "Differential modulation for two-way wireless communications: A perspective of differential network coding at the physical layer," *Trans. Commun.*, vol. 57, no. 10, pp. 2977–2987, Oct. 2009.
[26] A. Orsino *et al.*, "Effects of heterogeneous mobility on D2D and drone-assisted mission-critical MTC in 5G," *IEEE Commun. Mag.*, vol. 55, no. 2, pp. 79–87, Feb. 2017.
[27] N. Brahmi, O. N. C. Yilmaz, K. W. Helmersson, A. A. Ashraf, and J. Torsner, "Deployment strategies for ultra-reliable and low-latency communication in factory automation," in *Proc. IEEE Globecom Workshop*, Dec. 2017, pp. 1–6.
[28] "Common Public Radio Interface (CPRI) specifications V7.0," Oct. 2015, [Online]. Available: http://www.cpri.info/downloads/CPRI_v_7_0_2015-10-09.pdf
[29] S. Haykin, *Adaptive Filter Theory (1st Ed.)*. Englewood Cliffs, NJ, USA: Prentice-Hall, Inc., 1986.
[30] Y. Lee and H. W. Shieh, "Detection with erasure in relay for decode-and-forward cooperative communications," *IEEE Trans. Veh. Technol.*, vol. 62, no. 2, pp. 908–913, Feb. 2013.
[31] F. A. Onat, Y. Fan, H. Yanikomeroglu, and H. V. Poor, "Threshold-based relay selection for detect-and-forward relaying in cooperative wireless networks," *EURASIP J. Wireless Commun. Netw.*, vol. 2010, p. 1–9, 2010, doi: 10.1155/2010/721492.
[32] Y. Zhu, P. Y. Kam, and Y. Xin, "Differential modulation for decode-and-forward multiple relay systems," *Trans. Commun.*, vol. 58, no. 1, pp. 189–199, Jan. 2010.
[33] A. Alimohammad, S. Fard, B. Cockburn, and C. Schlegel, "An accurate and compact Rayleigh and Rician fading channel simulator," in *Proc. IEEE Veh. Technol. Conf.*, May 2008, pp. 409–413.
[34] L. A. Ekman, W. B. Kleijn, and M. N. Murthi, "Regularized linear prediction of speech," *IEEE Trans. Audio, Speech, Lang. Process.*, vol. 16, no. 1, pp. 65–73, Jan. 2008.
[35] J. Proakis and M. Salehi, *Digital Communications*. 5th ed. New York, NY, USA: McGraw-Hill, 2008.
[36] F. Danilo and H. Leib, "Detection techniques for fading multipath channels with unresolved components," *IEEE Trans. Inf. Theory*, vol. 44, no. 7, pp. 2848–2863, Nov. 1998.
[37] G. L. Turin "The characteristic function of Hermitian quadratic forms in complex normal variables," *Biometrika*, vol. 47, no. 1/2, pp. 199–201, 1960.
[38] M. Evgrafov, *Analytic Functions*. ser. Saunders mathematics books. Philadelphia, PA, USA: Saunders, 1966.
[39] S. V. Amari and R. B. Misra, "Closed-form expressions for distribution of sum of exponential random variables," *IEEE Trans. Rel.*, vol. 46, no. 4, pp. 519–522, Dec. 1997.
[40] H. W. Gould, *Combinatorial Identities: A Standardized Set of Tables Listing 500 Binomial Coefficient Summations*. Morgantown, WV, USA: Morgantown Printing and Binding, 1972.
[41] J. Riordan, *Combinatorial Identities*. Hoboken, NJ, USA: Wiley, 1968.

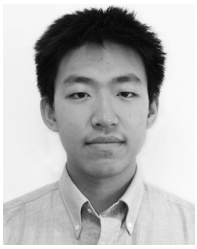

JUNQIAN ZHANG was born in Taiyuan, Shanxi, China, in 1989. He received the B.A.Sc. degree from the University of Toronto, Toronto, ON, Canada, in 2014, and the M.Eng. degree from McGill University, Montreal, QC, Canada, in 2017, both in electrical engineering. From 2014 to 2017, he was a Research Assistant with McGill University. His research interests include cooperative communication, relay networks, differential modulation systems, WDFDC receiver, and modeling of communication systems. He is currently a Systems Engineer in wireless communications group with Analog Devices, Inc., Toronto, ON, Canada, working on embedded system design for communication systems.

HARRY LEIB received the B.Sc. (*cum laude*) and M.Sc. degrees in electrical engineering from the Technion - Israel Institute of Technology, Haifa, Israel, in 1977 and 1984, respectively, and the Ph.D. degree in electrical engineering from the University of Toronto, Toronto, ON, Canada, in 1987.

During 1977–1984, he was with the Israel Ministry of Defense, working in Communication Systems. After completing his Ph.D. studies, he was with the University of Toronto as a Postdoctoral Research Associate and an Assistant Professor. Since September 1989, he has been with the Department of Electrical and Computer Engineering, McGill University, Montreal, QC, Canada, where he is currently a Full Professor. His current research activities are in the areas of digital communications, wireless communication systems, global navigation satellite systems, detection, estimation, and information theory.

Dr. Leib was an Editor for the IEEE TRANSACTIONS ON COMMUNICATIONS 2000–2013, and an Associate Editor for the IEEE TRANSACTIONS ON VEHICULAR TECHNOLOGY 2001–2007. He was a Guest Co-Editor for special issues of the IEEE JOURNAL ON SELECTED AREAS IN COMMUNICATION on "Differential and Noncoherent Wireless Communication" 2003–2005, and on "Spectrum and Energy Efficient Design of Wireless Communication Networks" 2012–2013. Since 2017, he has been the founding Editor-in-Chief for *AIMS Electronics and Electrical Engineering Journal*.